Printed ISSN 1330–0008
Online ISSN 1333–9125
CD ISSN 1333–8390
CODEN FIZAE4

STRUCTURAL, ELASTIC, ELECTRONIC AND LATTICE DYNAMIC PROPERTIES OF $GaP_xAs_ySb_{1-x-y}$ ALLOYS LATTICE MATCHED TO DIFFERENT SUBSTRATES

B. GHEBOULI[a,1], M. A. GHEBOULI[b] and M. FATMI[c]

[a]*Laboratory for Studying Surfaces and Interfaces of Solid Materials, University Ferhat Abbas, Sétif 19000, Algeria E-mail address: bghebouli@yahoo.fr*

[b]*Departement of Physics, University Center, Bordj-Bou-Arréridj 34000, Algeria*

[c]*Research Unit on Emerging Materials, University Ferhat Abbas, Sétif 19000, Algeria*

Received 17 July 2010; Accepted 9 February 2011
Online 2 May 2011

Information on the energy band gaps, the lattice parameter and the lattice matching to available substrates is a prerequisite for many practical applications. A pseudopotential plane-wave method, as implemented in the ABINIT code, is used to the $GaP_xAs_ySb_{1-x-y}$ quaternary alloy lattice matched to GaAs and InP substrates to predict their energy band gaps, elastic constants and lattice dynamic properties. The ranges of compositions for which the alloy is lattice-matched to GaAs and InP are determined. A very good agreement is obtained between the calculated values and the available experimental data of GaAs and $GaAs_{0.5}Sb_{0.5}$ parents. The compositional dependence of direct and indirect band gaps has been investigated. Note that a phase transition occurred at As composition of 0.018 and 0.576 for $GaP_xAs_ySb_{1-x-y}$ within InP and GaAs substrates. The static and high-frequency dielectric constants and refractive index are indeed inversely proportional (proportional) to the fundamental band gap for $GaP_xAs_ySb_{1-x-y}$ within InP (GaAs) substrates. We study the variation of elastic constants, the optical phonon frequencies (ω_{TO} and ω_{LO}) and the Born effective charge Z^* with As concentration.

PACS numbers: 61.72.Vv, 61.43.Bn UDC 538.911, 538.951

Keywords: structural properties, electronic properties, first principles calculations, lattice dynamic properties, Born effective charge, elastic properties

[1]Corresponding author

1. Introduction

Alloys formed by mixing the group III-V elements, having the properties of semiconductor materials with wide band gaps have been used for many device applications [1]. These semiconductors are used to produce commercially important high-performance electronic and optoelectronic devices and systems, such as light emitting devices covering many regions of the visible spectrum. The availability of quaternary alloys $GaP_xAs_ySb_{1-x-y}$ lattice matched to GaAs and InP substrates permits an extra degree of freedom by allowing independent control of the band gap, E_g, and the lattice constant, a_0. These compounds could lead to new semiconductor materials with desired band gaps over a continuous broad spectrum of energies [2 − 9]. Furthermore, the use of quaternary alloys enhances the experimental capability to investigate the effects of strain and piezoelectric fields in quantum wells [10].

In this work, we carried out a theoretical study of the energy band gaps, elastic, lattice dynamic and thermodynamic properties of the quaternary $GaP_xAs_ySb_{1-x-y}$, lattice matched to GaAs and InP substrates. This study of the quaternary alloys is calculated using the pseudo-potential plane-wave method as implemented in the ABINIT code. The calculations were performed over the entire composition range of x and y.

The paper is organized as follows: The theoretical framework within which all calculations have been performed is outlined in Section 2. In Section 3, we present and discuss the results of our study regarding the structural, elastic, electronic, lattice dynamic and thermodynamic properties of the quaternary $GaP_xAs_ySb_{1-x-y}$ alloys, lattice matched to GaAs and InP substrates. A conclusion is given in Section 4.

2. Computational method

The calculations were performed using the pseudo-potential plane-wave method as implemented in the ABINIT code [11] within the generalized gradient approximation (GGA) to the density functional theory (DFT). ABINIT computer code is a common project of the University Catholique of Louvain, Corning Incorporated, and other contributors. Only the outermost electrons of each atom were explicitly considered in the calculation. The effects of the inner electrons and the nucleus were described within the Hartwigzen-Goedecker-Hutter scheme [12] to generate the norm-conserving nonlocal pseudo-potentials. The Brillouin zone integrations were replaced by discrete summations over a special set of k-points, using the standard k-point technique of Monkhorst and Pack [13] where the k-point mesh used is $(8 \times 8 \times 8)$. The plane-wave energy cutoff to expand the wave functions is set to be 90 Hartree (1 Hartree = 27.211396 eV). For the treatment of the disordered ternary alloy, we used the VCA [14], in which the alloys pseudo-potentials are constructed within a first-principles VCA scheme. Recently, Marques et al. [15] reported a linear behavior of the lattice parameter of $Al_xGa_yIn_{1-x-y}N$ as a function of the compo-

sition x and y. Thus, the Vegard's rule has been assumed for the calculation of the lattice constant of quaternary alloys under study

$$a_{\mathrm{VCA}} = x a_{\mathrm{GaP}} + y a_{\mathrm{GaAs}} + (1-x-y) a_{\mathrm{GaSb}}\,. \tag{1}$$

3. Results and discussion

3.1. Structural properties

The GaX semiconducting alloys crystallize in the zinc-blende structure with a space group F-43m. The Ga and X atoms are located at the origin and (1/4, 1/4, 1/4), respectively. The equilibrium lattice parameter is computed from the structural optimization, using the Broyden-Fletcher-Goldfarb-Shanno minimization [16−19]. The lattice matching conditions for $\mathrm{GaP}_x\mathrm{As}_y\mathrm{Sb}_{1-x-y}$ quaternary systems on the GaAs and InP substrates, as shown in Fig. 1, are: $y = 1 - 1.457x$ and $y = 0.51 - 1.457x$. The range for which this compound is lattice matched to GaAs substrate is larger than that corresponding to the InP one. The results of lattice parameters a_0 are given in Table 1 for different composition rates x and y. Figure 2 shows the lattice parameter plotted versus As fraction y.

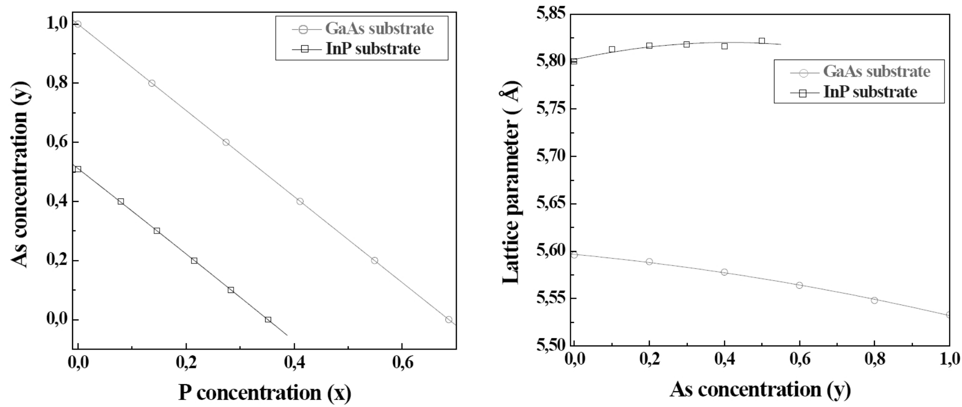

Fig. 1 (left). Lattice matching conditions of $\mathrm{GaP}_x\mathrm{As}_y\mathrm{Sb}_{1-x-y}$ *quaternary systems on the* GaAs and InP substrates.

Fig. 2. Relaxed lattice parameter of $\mathrm{GaP}_x\mathrm{As}_y\mathrm{Sb}_{1-x-y}$ /GaAs(lnP) *structures as a function of* As *composition* y*.*

The lattice parameter of the $\mathrm{GaP}_x\mathrm{As}_y\mathrm{Sb}_{1-x-y}$ lattice matching to the GaAs (InP) substrate decreases (increases) when the As composition y is enhanced. We observe that the lattice parameter calculated within InP substrate is greater than that corresponding to the GaAs one. The deviation from the linear dependence is distinct. An analytical relation for the compositional dependence of $\mathrm{GaP}_x\mathrm{As}_y\mathrm{Sb}_{1-x-y}$

lattice parameter is given by the quadratic fit for GaAs and InP substrates,

$$a = 5.596 - 0.037y - 0.027y^2, \qquad \text{and} \qquad a = 5.8 + 0.086y - 0.1y^2\,. \qquad (2)$$

TABLE 1: The calculated lattice constant a_0, elastic constants C_{11}, C_{12} and C_{44} and bulk modulus B of $GaP_xAs_ySb_{1-x-y}$ lattice matched to GaAs and InP substrates at zero pressure.

Material	a_0(Å)	C_{11}	C_{12}	C_{44}	B
$GaP_{0.686}Sb_{0.314}$/GaAs	5.596	121.65	53.6	59.88	76.28
$GaP_{0.549}As_{0.2}Sb_{0.251}$/GaAs	5.589	121.2	53.3	59.89	75.93
$GaP_{0.419}As_{0.4}Sb_{0.181}$/GaAs	5.578	121.98	53.57	60.38	76.37
$GaP_{0.274}As_{0.6}Sb_{0.126}$/GaAs	5.564	122.78	53.82	60.93	76.8
$GaP_{0.137}As_{0.8}Sb_{0.063}$/GaAs	5.548	124.66	54.92	62.18	78.16
GaAs					
This work	5.533	125.7	55.27	62.95	78.74
Experiment	[a]5.653	[e]122	[e]57	[e]60	[b]79, [c]76
Other works	[b]5.51, [c]5.55	[d]123	[d]49	[d]64	–
$GaP_{0.352}Sb_{0.648}$/InP	5.8	105.37	46.76	51.31	66.29
$GaP_{0.283}As_{0.1}Sb_{0.617}$/InP	5.813	102.85	45.46	50.23	64.59
$GaP_{0.215}As_{0.2}Sb_{0.585}$/InP	5.817	101.8	44.87	49.7	63.84
$GaP_{0.146}As_{0.3}Sb_{0.554}$/InP	5.818	100.75	44.53	49.24	63.27
$GaP_{0.08}As_{0.4}Sb_{0.52}$/InP	5.816	100	44.25	49	62.83
$GaAs_{0.5}Sb_{0.5}$/InP					
This work	5.817	99	44.35	48.7	62.56
Other works	–	[f]109.5	[f]47.2	[f]50.6	–

[a][25], [b][26], [c][27], [d][28], [e][29], [f][30]

3.2. Elastic properties

The elastic constants are important parameters that describe the response to an applied macroscopic stress. In Table 1, we show the calculated elastic constants, C_{11}, C_{12} and C_{44}, and bulk modulus B of $GaP_xAs_ySb_{1-x-y}$ structure lattice matched to GaAs and InP at zero pressure and for various compositions y in the range $(0-1)$ and $(0-0.5)$. For comparison are also given the available experimental data and other results for GaAs and $GaAs_{0.5}Sb_{0.5}$ parents. To the best of our knowledge, no experimental data have been reported for the elastic constants of $GaP_xAs_ySb_{1-x-y}$ in the composition range considered for GaAs and InP substrates. In Fig. 3, we depict the composition dependence of the elastic constants (C_{11}, C_{12} and C_{44}) and the bulk modulus B of $GaP_xAs_ySb_{1-x-y}$ lattice

matched to GaAs and InP substrates. We observe a quadratic dependence in all curves in the considered range of composition for both substrates. It is easy to observe that the variation on elastic constants C_{ij} and bulk modulus B is weaker when the concentration y is enhanced for both substrates. We remark that all these parameters given for InP substrate are lower than those corresponding to the GaAs one. The mechanical stability requires that elastic constants satisfy the well-known Born stability criteria [20],

$$K = \frac{1}{3}(C_{11} + 2C_{12} + P) > 0, \quad G = \frac{1}{2}(C_{11} - 2C_{12} - 2P) > 0, \quad G' = C_{44} - P > 0 \,. \quad (3)$$

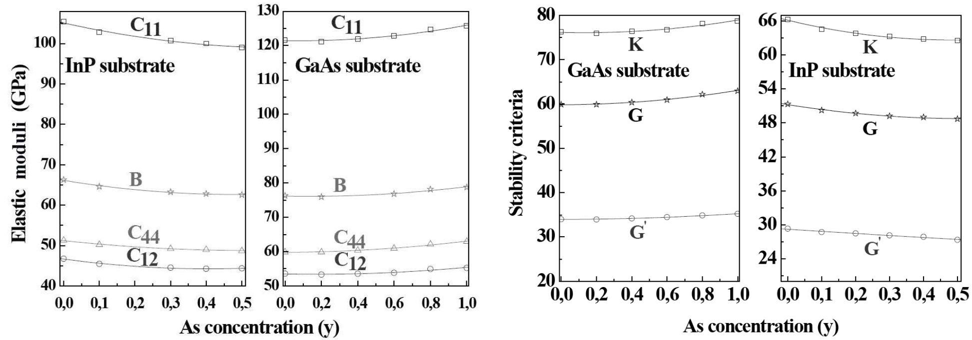

Fig. 3 (left). As composition dependence of the elastic constants and bulk modulus in $GaP_xAs_ySb_{1-x-y}$ /GaAs(lnP) *structures.*

Fig. 4. Stability criteria of $GaP_xAs_ySb_{1-x-y}$ /GaAs(lnP) *structures as a function of* As *concentration* y *at zero pressure.*

In Fig. 4, we show the dependence of stability criteria of $GaP_xAs_ySb_{1-x-y}$ compounds with As concentration y at zero pressure for the two substrates. From our calculated C_{ij} values, these compounds are mechanically stable.

From the theoretical elastic constants, we computed the elastic wave velocities. The single-crystal elastic wave velocities in different directions are given by the resolution of the Cristoffel equation [21],

$$(C_{ijkl} \cdot n_i \cdot n_k - \rho v^2 \cdot \delta_{il}) u_l = 0 \quad (4)$$

where, C_{ijkl} is the single-crystal elastic constant tensor, n is the propagation direction, ρ is the density of the material, u is the wave polarization and v is the wave velocity. The solutions of this equation are of two types: a longitudinal wave with polarization parallel to the direction of propagation v_l and two shear waves v_{T1} and v_{T2} with polarization perpendicular to n. The calculated elastic wave velocities along the [100], [110] and [111] directions for $GaP_xAs_ySb_{1-x-y}$/GaAs(InP) compounds at zero pressure are shown in Table 2. At zero pressure, longitudinal waves are fastest along the [111] direction and shear waves are slowest along [111] for both substrates. We remark that all wave velocities calculated within the GaAs substrates are greater than those corresponding to the InP substrates.

TABLE 2: The elastic wave velocities of $GaP_xAs_ySb_{1-x-y}$ *lattice matched to* GaAs *and* InP *substrates in* (ms^{-1}) *for different propagation directions at equilibrium.*

Material	v_L^{100}	v_T^{100}	v_L^{110}	v_{T1}^{110}	v_{T2}^{110}	v_L^{111}	v_T^{111}
$GaP_{0.686}Sb_{0.314}$/GaAs	4983	3496	5488	3727	3496	5646	2950
$GaP_{0.549}As_{0.2}Sb_{0.251}$/GaAs	4907	3449	5407	3673	3449	5563	2909
$GaP_{0.419}As_{0.4}Sb_{0.181}$/GaAs	4864	3422	5360	3642	3422	5516	2885
$GaP_{0.274}As_{0.6}Sb_{0.126}$/GaAs	4794	3377	5285	3593	3377	5439	2847
$GaP_{0.137}As_{0.8}Sb_{0.063}$/GaAs	4757	3360	5253	3558	3360	5408	2825
GaAs							
This work	4707	3331	5200	3523	3331	5355	2799
Experiment	[b]4784	[b]3350	[b]5289	–	–	[b]5447	[b]5447
Other works	[a]4690	[a]3380	[a]5020	–	–	[a]5350	[a]2820
$GaP_{0.352}Sb_{0.648}$/InP	4404	3073	4842	3285	3073	4980	2597
$GaP_{0.283}As_{0.1}Sb_{0.617}$/InP	4344	3036	4778	3245	3036	4914	2566
$GaP_{0.215}As_{0.2}Sb_{0.585}$/InP	4307	3009	4735	3221	3009	4869	2545
$GaP_{0.146}As_{0.3}Sb_{0.554}$/InP	4265	2981	4691	3186	2981	4825	2519
$GaP_{0.08}As_{0.4}Sb_{0.52}$/InP	4230	2961	4655	3158	2961	4789	2499
$GaAs_{0.5}Sb_{0.5}$/InP							
This work	4177	2930	4606	3104	2930	4741	2464
Other works	[c]4490	[c]3050	–	–	–	[d]5400	[d]2800

[a][28], [b][29], [c][30], [d][31]

Once the elastic constants are determined, we compare our results with experiments, or predict what experiments would yield for the elastic constants. For a cubic crystal, the isotropic bulk modulus B is given by

$$B = \frac{1}{3}(C_{11} + 2C_{12})\,. \tag{5}$$

We also calculated Young's modulus E and Poisson's ratio ν which are frequently measured for polycrystalline materials when investigating their hardness. These quantities are related to the bulk modulus and the shear modulus by the following equations [22],

$$E = \frac{9BG}{3B+G}, \qquad \nu = \frac{3B-E}{6B}\,, \tag{6}$$

where, $G = (G_R + G_V)/2$. The shear moduli G_R and G_V, Young's modulus E and Poisson's ratio ν for $GaP_xAs_ySb_{1-x-y}$/GaAs(InP) structures, calculated from the elastic constants, are listed in Table 3.

TABLE 3: The calculated shear moduli G_R and G_V, Young's modulus E, and Poissons's ratio, ν, of $GaP_xAs_ySb_{1-x-y}$ lattice matched to GaAs and InP substrates at zero pressure.

Material	Shear modulus G_R (GPa)	Shear modulus G_V (GPa)	Young's modulus E (GPa)	Poisson's ratio ν
$GaP_{0.686}Sb_{0.314}$/GaAs	45.92	49.54	118.48	0.241
$GaP_{0.549}As_{0.2}Sb_{0.251}$/GaAs	45.87	49.51	118.31	0.24
$GaP_{0.419}As_{0.4}Sb_{0.181}$/GaAs	46.22	49.91	119.20	0.239
$GaP_{0.274}As_{0.6}Sb_{0.126}$/GaAs	46.62	50.35	120.17	0.239
$GaP_{0.137}As_{0.8}Sb_{0.063}$/GaAs	47.35	51.26	122.21	0.239
GaAs	47.87	51.87	123.52	0.238
$GaP_{0.352}Sb_{0.648}$/InP	39.46	42.51	101.94	0.244
$GaP_{0.283}As_{0.1}Sb_{0.617}$/InP	38.63	41.62	99.72	0.243
$GaP_{0.215}As_{0.2}Sb_{0.585}$/InP	38.28	41.21	98.74	0.242
$GaP_{0.146}As_{0.3}Sb_{0.554}$/InP	37.86	40.79	97.72	0.243
$GaP_{0.08}As_{0.4}Sb_{0.52}$/InP	37.60	40.55	97.09	0.241
$GaAs_{0.5}Sb_{0.5}$/InP	45.14	45.49	112.22	0.238

3.3. Calculation of the Debye temperature

Having calculated the Young's modulus E, the bulk modulus B and the shear modulus G, one can calculate the Debye temperature, which is an important fundamental parameter closely related to many physical properties such as elastic constants, specific heat and melting temperature. At low temperature, the vibrational excitations arise solely from acoustic mode. Hence, at low temperature the Debye temperature calculated from elastic constants is the same as that determined from specific heat measurements. One of the standard methods to calculate the Debye temperature θ_D is from elastic data, since it may be estimated from the average sound velocity v_m by the equation [23]

$$\theta_D = \frac{h}{k_B}\left(\frac{3n}{4\pi V_a}\right)^{1/3} v_m \, , \tag{7}$$

where h is the Planck constant, k_B the Boltzmann constant and V_a the atomic volume. The average sound velocity in the polycrystalline material is given by [24]

$$v_m = \left[\frac{1}{3}\left(\frac{2}{v_l^2} + \frac{1}{v_t^2}\right)\right]^{-1/3} , \tag{8}$$

where, v_l and v_t are the longitudinal and transverse sound velocities of an isotropic aggregate obtained using the shear modulus G and the bulk modulus B from Navier's equations [22],

$$v_l = \left(\frac{3B+4G}{3\rho}\right)^{1/2}, \qquad v_t = \left(\frac{G}{\rho}\right)^{1/2}. \tag{9}$$

In Table 4 are given the calculated sound velocities as well as the density of $GaP_xAs_ySb_{1-x-y}$/GaAs(InP) structures We plot the dependence of the Debye temperature with As concentration y in Fig. 5. We note that the Debye temperature decreases with increasing As composition y. The Debye temperature of $GaP_xAs_ySb_{1-x-y}$ given within the InP substrate is lower than that corresponding to the GaAs one. The Debye temperature is greater in material having greater bulk modulus for the same conditions.

TABLE 4: The calculated density ρ, the longitudinal, transverse and average sound velocity v_l, v_t and v_m calculated from polycrystalline elastic modulus of $GaP_xAs_ySb_{1-x-y}$ *lattice matched to* GaAs *and* InP *substrates at zero pressure.*

Material	ρ (g cm^{-3})	v_l (m s^{-1})	v_t (m s^{-1})	v_m (m s^{-1})
$GaP_{0.686}Sb_{0.314}$/GaAs	4.8975	5345	3122	3462
$GaP_{0.549}As_{0.2}Sb_{0.251}$/GaAs	5.0328	5265	3078	3413
$GaP_{0.419}As_{0.4}Sb_{0.181}$/GaAs	5.1558	5219	3053	3385
$GaP_{0.274}As_{0.6}Sb_{0.126}$/GaAs	5.3413	5146	3012	3340
$GaP_{0.137}As_{0.8}Sb_{0.063}$/GaAs	5.5070	5111	2992	3317
GaAs	5.6724	5059	2964	3287
$GaP_{0.352}Sb_{0.648}$/InP	5.4309	4719	2747	3047
$GaP_{0.283}As_{0.1}Sb_{0.617}$/InP	5.448	4655	2713	3010
$GaP_{0.215}As_{0.2}Sb_{0.585}$/InP	5.487	4614	2691	2985
$GaP_{0.146}As_{0.3}Sb_{0.554}$/InP	5.5375	4570	2664	2955
$GaP_{0.08}As_{0.4}Sb_{0.52}$/InP	5.5874	4535	2644	2933
$GaAs_{0.5}Sb_{0.5}$/InP	5.6716	4484	2609	2895

3.4. Electronic properties

The band structures of $GaP_xAs_ySb_{1-x-y}$ lattice matched to GaAs and InP were calculated through the high-symmetry points Γ, X and L in the Brillouin zone. For example, we show the band structures of the parents alloys $GaAs_{0.51}Sb_{0.49}$, $GaP_{0.352}Sb_{0.648}$, $GaP_{0.686}Sb_{0.314}$ and GaAs with direct and indirect band gaps Γ-Γ and Γ-L in Fig. 6. The direct band gaps Γ-Γ, L-L, X-X and indirect band gaps Γ-L,

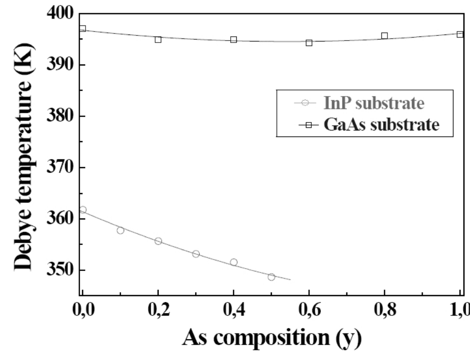

Fig. 5. Dependence of the Debye temperature in $GaP_xAs_ySb_{1-x-y}$ /GaAs(lnP) *structures on* As *composition.*

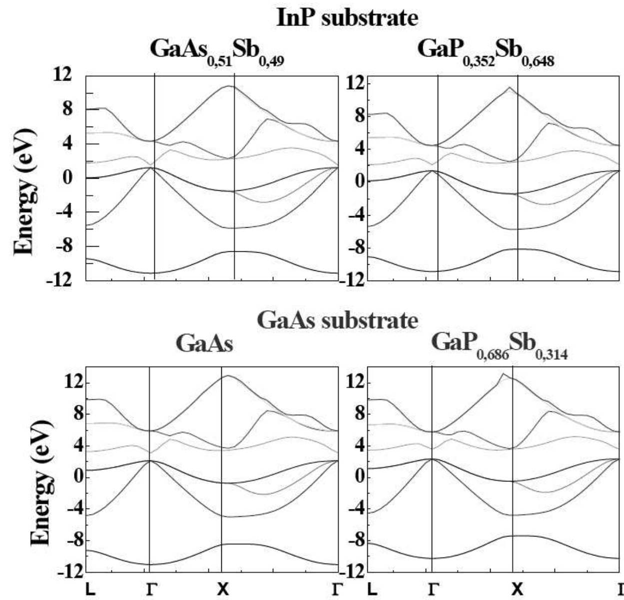

Fig. 6. Band structures of $GaAs_{0.51}Sb_{0.49}$, $GaP_{0.352}Sb_{0.643}$, GaAs *and* $GaP_{0.636}Sb_{0.314}$ *parents of* $GaP_xAs_ySb_{1-x-y}$ *at equilibrium.*

Γ-X of $GaP_xAs_ySb_{1-x-y}$/GaAs(InP) at zero pressure are shown in Table 5. The As composition energy variations of the conduction band edges at Γ, X and L with respect to the top of the valence band are obtained. Results are plotted in Fig. 7, which show the dependence of direct and indirect band-gap energies in the lattice matched $GaP_xAs_ySb_{1-x-y}$/GaAs(InP) structures on the As y content. Note that a phase transition Γ-L to Γ-Γ occurred at As composition of 0.018 for InP substrate and Γ-Γ to Γ-L at 0.576 for the GaAs one. The $GaP_xAs_ySb_{1-x-y}$/GaAs shows a narrower band gap than that observed in $GaP_xAs_ySb_{1-x-y}$/InP. We obtained the

TABLE 5: The calculated values of band gaps of $GaP_xAs_ySb_{1-x-y}$ *lattice matched to* GaAs *and* InP *substrates at equilibrium.*

Material	$E_{\Gamma-\Gamma}$	E_{L-L}	E_{X-X}	$E_{L-\Gamma}$	$E_{X-\Gamma}$
$GaP_{0.686}Sb_{0.314}$/GaAs	1.24	2.32	4.06	1.1	1.22
$GaP_{0.549}As_{0.2}Sb_{0.251}$/GaAs	1.17	2.31	4.07	1.1	2.24
$GaP_{0.419}As_{0.4}Sb_{0.181}$/GaAs	1.1	2.32	4.09	1.11	1.26
$GaP_{0.274}As_{0.6}Sb_{0.126}$/GaAs	1.08	2.34	4.11	1.12	1.27
$GaP_{0.137}As_{0.8}Sb_{0.063}$/GaAs	1.04	2.36	4.14	1.14	1.29
GaAs					
This work	1	2.38	4.16	1.16	1.31
Experiment	[a]1.41	–	–	[c]1.72	[c]1.81
Other works	[b]0.92, [b]1.01	–	–	[d]1.15	[d]1.34
$GaP_{0.352}Sb_{0.648}$/InP	0.742	1.96	3.816	0.727	1
$GaP_{0.283}As_{0.1}Sb_{0.617}$/InP	0.609	1.88	3.78	0.664	0.998
$GaP_{0.215}As_{0.2}Sb_{0.585}$/InP	0.511	1.84	3.772	0.622	1.01
$GaP_{0.146}As_{0.3}Sb_{0.554}$/InP	0.441	1.81	3.773	0.595	1.015
$GaP_{0.08}As_{0.4}Sb_{0.52}$/InP	0.382	1.79	3.778	0.578	1.024
$GaAs_{0.5}Sb_{0.5}$/InP	0.305	1.75	3.77	0.545	1.02

[a][25], [b][26], [c][32], [d][33]

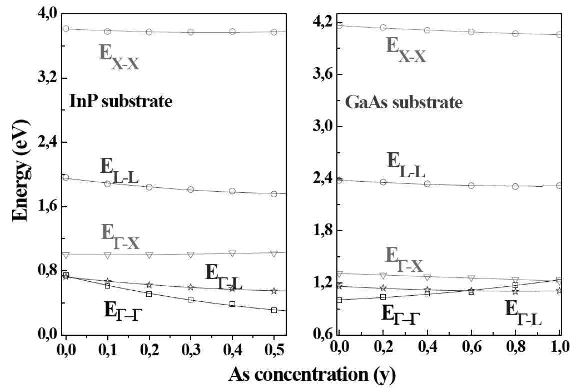

Fig. 7. Direct Γ-Γ, *L-L and X-X and indirect* Γ*-L and* Γ*-X band-gap energies in* $GaP_xAs_ySb_{1-x-y}$/GaAs(InP) *quaternary alloys as a function of* As *concentration* y.

following analytical expressions by fitting our energy gaps data using the least-squares procedure:

GaAs substrate,

$$E_\Gamma^\Gamma = 1+0.109y+0.12y^2, \quad E_\Gamma^X = 1.31-0.09y+0y^2, \quad E_\Gamma^L = 1.16-0.14y+0.08y^2,$$

$$E_L^L = 2.38 - 0.15y + 0.084y^2, \quad E_X^X = 4.16 - 0.14y + 0.04y^2; \qquad (10a)$$

InP substrate,

$$E_\Gamma^\Gamma = 0.73-1.22y+0.778y^2, \quad E_\Gamma^X = 0.998+0.007y+0.09y^2, \quad E_\Gamma^L = 0.72-0.56y+0.44y^2,$$

$$E_L^L = 1.95 - 0.64y + 0.52y^2, \quad E_X^X = 3.8 - 0.23y + 0.34y^2. \qquad (10b)$$

3.5. Lattice dynamic properties

The longitudinal and transversal optical phonon frequencies, referred to ω_{L0} and ω_{T0}, respectively, of $GaP_xAs_ySb_{1-x-y}$/GaAs(InP) at various compositions y are numerically listed in Table 6. For comparison, also shown are the existing experimental and theoretical data in the literature for GaAs compound. The

TABLE 6. Born effective charge, the longitudinal optical (LO) and transverse optical (TO) phonon frequencies, the static and high frequency dielectric constants and refractive index of $GaP_xAs_ySb_{1-x-y}$ *lattice matched to* GaAs *and* InP *substrates for different* As *concentration* y *at equilibrium.*

Material	Z^*	ω_{LO} (cm^{-1})	ω_{LO} (cm^{-1})	ϵ_0	ϵ_∞	n
$GaP_{0.686}Sb_{0.314}$/GaAs	1.962	304.27	290.6	11.10	10.133	3.138
$GaP_{0.549}As_{0.2}Sb_{0.251}$/GaAs	1.983	300.24	286.43	11.13	10.14	3.14
$GaP_{0.419}As_{0.4}Sb_{0.181}$/GaAs	2	298.73	284.77	11.151	10.133	3.183
$GaP_{0.274}As_{0.6}Sb_{0.126}$/GaAs	2.032	294.47	280.03	11.296	10.215	3.196
$GaP_{0.137}As_{0.8}Sb_{0.063}$/GaAs	2.056	292.54	277.71	11.520	10.382	3.222
GaAs						
This work	2.08	290.53	275.26	11.757	10.553	3.248
Experiment	[b]2.16	[d]285	[d]267	[e]12.9	[b]10.9	–
Other works	[c]1.94	[a]292.1	[a]268.7	–	–	–
$GaP_{0.352}Sb_{0.648}$/InP	1.832	262.33	254.39	12.611	11.859	3.443
$GaP_{0.283}As_{0.1}Sb_{0.617}$/InP	1.847	259.24	251.66	13.272	12.508	3.536
$GaP_{0.215}As_{0.2}Sb_{0.585}$/InP	1.86	257.56	250.12	13.882	13.092	3.618
$GaP_{0.146}As_{0.3}Sb_{0.554}$/InP	1.876	255.9	248.63	14.340	13.536	3.679
$GaP_{0.08}As_{0.4}Sb_{0.52}$/InP	1.893	254.82	247.58	14.757	13.931	3.732
$GaAs_{0.5}Sb_{0.5}$/InP	1.899	253.3	246.25	15.314	14.474	3.804

[a][34], [b][35], [c][36], [d][37], [e][31]

agreement between our results and experiment as regards ω_{L0} and ω_{T0} of GaAs is better than 1.9% and 2.9%. No comparison has been made in the considered composition range, as there are no known data available to date to the best of our knowledge. The variation of the frequencies of the LO and TO phonons in $GaP_xAs_ySb_{1-x-y}$/GaAs(InP) quaternary alloys as a function of the As concentration y is plotted in Fig. 8. One obtains for ω_{L0} and ω_{T0}:

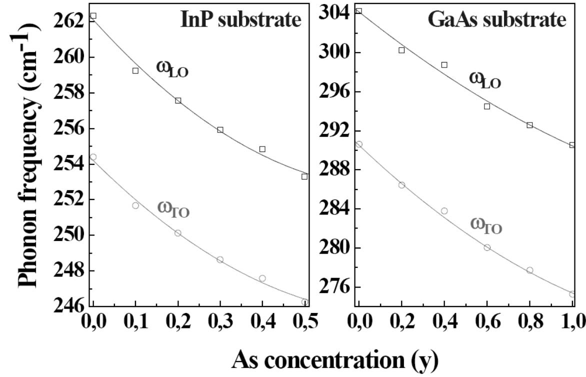

Fig. 8. Frequencies of the longitudinal optical (LO) and transversal optical (TO) phonons in $GaP_xAs_ySb_{1-x-y}$/GaAs(InP) *quaternary alloys as function of* As *concentration y.*

For InP substrate

$$\omega_{L0} = 262.09 - 26.3y + 18.28y^2, \qquad \omega_{T0} = 254.19 - 23.53y + 15.97y^2; \qquad (11a)$$

For GaAs substrate

$$\omega_{L0} = 304.15 - 20y + 6.49y^2, \qquad \omega_{T0} = 290.5 - 20.77y + 5.64y^2 . \qquad (11b)$$

These expressions may be used to predict the LO and TO phonon frequencies for any As concentration y in the considered range for $GaP_xAs_ySb_{1-x-y}$ /GaAs (InP) structures. Note also that both ω_{L0} and ω_{T0} change non-linearly and decrease as the composition y increases. For the same concentration y, ω_{L0} is greater than ω_{T0}. The frequencies of the LO and TO phonons of $GaP_xAs_ySb_{1-x-y}$ within the InP substrate are lower than those corresponding to the GaAs one for the same concentration.

A good knowledge of the full electronic structure is an essential feature in order to get the best understanding of the optical properties of semiconductors. Thus, the refractive index which is essential in the design of heterostructure lasers, in optoelectronic devices as well as in solar cell applications has been estimated according to the relation $\epsilon(\infty) = n^2$. The knowledge of the dielectric constants makes it possible to proceed with the calculations of the refractive index. The static and high-frequency dielectric constants $\epsilon(0)$ and $\epsilon(\infty)$ have been calculated at various

As concentrations y, for the lattice matched $GaP_xAs_ySb_{1-x-y}$/GaAs(InP) structures. Our results are depicted in Table 6. For the fact that both experimental and theoretical data regarding n, $\epsilon(\infty)$ and $\epsilon(0)$ for $GaP_xAs_ySb_{1-x-y}$ lattice matched to GaAs and InP were not available, our results are predictions and may serve for reference. The variations of both static and high frequency dielectric constants as a function of As composition y are plotted in Fig. 9. The high-frequency dielectric and static dielectric constants increase monotonously with increasing As concentration y. These parameters are greater in the $GaP_xAs_ySb_{1-x-y}$ lattice matched to GaAs substrate than those corresponding to the InP one at the same value of As content. The dependence of the refractive index with As concentration y is shown in Fig. 10 for both substrates. The refractive index increases monotonously with increasing As composition. In order to provide analytical expressions for $\epsilon(\infty)$, $\epsilon(0)$ and n of the material of interest, the data obtained by our calculations were found

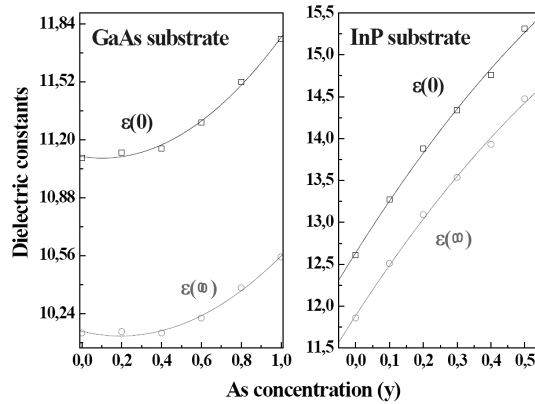

Fig. 9. Static and high frequency dielectric constants as a function of As *concentration y for the lattice matched* $GaP_xAs_ySb_{1-x-y}$/GaAs(InP) *structures.*

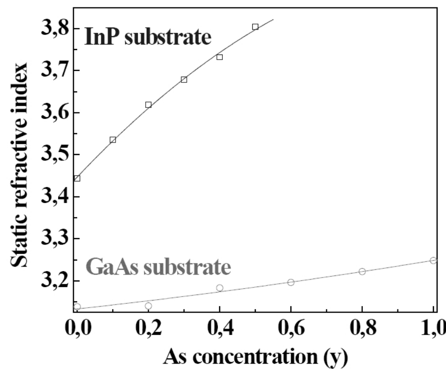

Fig. 10. Dependence of the static refractive index in $GaP_xAs_ySb_{1-x-y}$ /GaAs(lnP) *structures on* As *concentration.*

by a least squares procedure to fit best the following relations:

For InP substrate,

$$\epsilon(0) = 12.63 + 6.42y - 2.3y^2, \quad \epsilon(\infty) = 11.88 + 6.23y - 2.29y^2, \quad n = 3.44 + 0.89y - 0.39y^2; \tag{12a}$$

For GaAs substrate,

$$\epsilon(0) = 11.1 - 0.16y + 0.82y^2, \quad \epsilon(\infty) = 10.16 - 0.26y + 0.67y^2, \quad n = 3.13 + 0.09y - 0.023y^2. \tag{12b}$$

These expressions may be useful for obtaining $\epsilon(\infty)$, $\epsilon(0)$ and n for any y concentration in the considered range for $GaP_xAs_ySb_{1-x-y}$ alloy lattice matched to GaAs and InP.

In Table 6 are listed the calculated Born effective charges for various compositions y for $GaP_xAs_ySb_{1-x-y}$/GaAs(InP) structures. In Fig. 11, the absolute values of the calculated Born effective charges Z^* are plotted as a function of the As concentration y. The value of Z^* increases monotonously with increasing As content y. The agreement between our results and experiment as regards Z^* of GaAs is better than 3.7%. A quadratic fit to our data for both InP and GaAs substrates gives, respectively,

$$Z^* = 1.96 + 0.226 + 0.02y^2, \qquad Z^* = 1.83 + 0.009 - 0.02y^2. \tag{13}$$

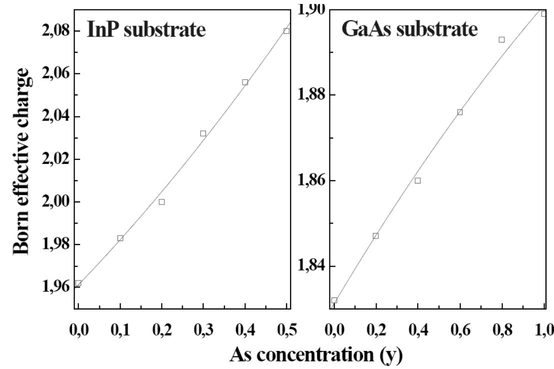

Fig. 11. Dependence of the Born effective charge in $GaP_xAs_ySb_{1-x-y}$ /GaAs(lnP) *structures on* As *concentration.*

4. Conclusion

We study the composition dependence of energy band gaps, elastic and dielectric constants of $GaP_xAs_ySb_{1-x-y}$ quaternary alloys, lattice matched to GaAs and InP substrates, by means of the pseudo-potential plane-wave method as implemented in the ABINIT code. Based on the calculated lattice constants, we predicted the ranges of compositions for which GaPAsSb is lattice matched to GaAs and InP substrates. Within the GaAs substrate, this compound shows a narrower band

gap than that corresponding to the InP one. Very good agreement was obtained between the band gap prediction and available experimental data for the GaAs parent. Our findings indicate that the high-frequency and the static dielectric constants increase monotonically with increasing As concentration y in the considered range. The expressions derived for the direct and indirect energy band gaps, static and high frequency dielectric constants as a function of As concentrations y are useful for tailoring electric and opto-electric devices based on cubic $GaP_xAs_ySb_{1-x-y}$ quaternary alloys. Due to the lack of experimental and theoretical data regarding the refractive index, high frequency, static dielectric constants and Born effective charge, our results are predictions and may serve as reference for future experimental work.

Acknowledgements

This work is supported by LESIMS Laboratory, University of Sétif (Algeria).

References

[1] I. Vurgaftman, J. R. Meyer and I. R. Ram-Mohan, J. Appl. Phys. **89** (2001) 5815.

[2] J. W. Orton and C. T. Foxon, Rep. Prog. Phys. **61** (1998) 1.

[3] S. C. Jain, M. Willander, J. Narayan and R. Van Overstraelen, J. Appl. Phys. **87** (2000) 965.

[4] K. Kassali and N. Bouarissa, Microelectron. Eng. **54** (2000) 277.

[5] I. Vurgaftman and J. R. Meyer, J. Appl. Phys. **94** (2003) 3675.

[6] S. Nakamura, Semiconduct. Sci. Technol. **14** (1999) R27.

[7] P. Kung and M. Razegui, Opt. Rev. **8** (2000) 201.

[8] M. Asif Khan, J. N. Kusnia, D. T. Olson, W. J. Schaff, J. W. Burm and M. S. Shur, Appl. Phys. Lett. **65** (1994) 1121.

[9] C. I. H. Ashby, C. C. Willan, J. Han, N. A. Missert, P. P. Provencio, D. M. Follstaedt, G. M. Peake and L. Griego, Appl. Phys. Lett. **77** (2000) 3233.

[10] F. G. McIntosh, K. S. Boutros, J. C. Roberts, S. M. Bedair, E. L. Piner and N. A. El-Masry, Appl. Phys. Lett. **68** (1996) 40.

[11] The ABINIT computer code is a common project of the Université Catholique de Louvain, Corning Incorporated and other contributors. Available online at: http://www.abinit.org.

[12] C. Hartwigsen, S. Goedecker and J. Hutter, Phys. Rev. B **58** (1998) 3641.

[13] H. J. Monkhorst and J. D. Pack, Phys. Rev. B **13** (1976) 5189.

[14] L. Nordheim, Ann. Phys. (Leipzig) **9** (1931) 607.

[15] M. Marques, L. K. Teles, L. M. R. Scolfaro, J. R. Leite, J. Furthmuller and F. Bechstedt, Appl. Phys. Lett. **83** (2003) 890.

[16] C. G. Broyden, J. Inst. Math. Appl. **6** (1970) 222.

[17] R. Fletcher, Comput. J. **13** (1970) 317.

[18] D. Goldfarb, Math. Comput. **24** (1970) 23.

[19] D. F. Shanno, Math. Comput. **24** (1970) 647.

[20] G. V. Sin'ko and A. Smirnov, J. Phys. Condens. Matter **14** (2002) 6989.

[21] O. L. Anderson, J. Phys. Chem. Solids **24** (1963) 909.

[22] M. W. Barsoum, T. El-Raghi, W. D. Porter, H. Wang and S. Chakraborty, J. Appl. Phys. **88** (2000) 6313.

[23] P. Wachter, M. Filzmoser and J. Rebisant, Physica B **293** (2001) 199.

[24] O. L. Anderson, J. Phys. Chem. Solids **24** (1963) 909.

[25] O. Madelung (ed.), *Semiconductors, Group IV Elements and III-V Compounds*, Landolt-Bornstein, New Series, Group III, vol. 17, Pt. a, Springer, Berlin (1991).

[26] R. Miotto and G. P. Srivastava, Phys. Rev. B **59** (1999) 3008.

[27] A. DalCorso, A. Pasquarello, A. Baldereschi and R. Car, Phys. Rev. B **53** (1996) 1180.

[28] N. Chimot, J. Even, H. Folliot and S. Loualiche, Physica B **364** (2005) 263.

[29] O. Madelung, M. Schulz and H. Weiss (eds.), *Landolt-Bornstein Numerical Data and functional Relationships in Science and Technology*, vol. 17, Springer, Berlin, Heidelberg, New York (1982).

[30] Nadir Bouarissa, Materials Chem. Phys. **100** (2006) 41.

[31] M. Levinshtein and S. Rumyantsev, M. Shur (Eds.), *Handbook Series on Semiconductor Parameters*, vol. 2, World Scientific, Singapore (1999) (and references cited therein).

[32] D. E. Aspnes, C. G. Olson and D. W. Lynch, Phys. Rev. Lett. **37** (1976) 766.

[33] S. Saib and N. Bouarissa, Solid State Electronics **50** (2006) 763.

[34] D. J. Lockwood, Guolin Yu and N. L. Rowell, Solid State Communications **136** (2005) 404.

[35] P. Vogl, J. Phys. C **11** (1978) 251.

[36] H. Baaziza, Z. Charifi and N. Bouarissa, Materials Letters **60** (2006) 39.

[37] Sadao Adachi, *Properties of Group-IV, III-V and II-VI Semiconductors*, Gunm University Japan (2005).

STRUKTURNA, ELASTIČNA, ELEKTRONSKA I REŠETKINA SVOJSTVA LEGURA $GaP_xAs_ySb_{1-x-y}$ S REŠETKAMA PRILEŽNIM DVJEMA PODLOGAMA

Podaci o energijskim procijepima, parametrima rešetke i priležívanju na dostupne podloge je preduvjet mnogin primjenama. Rabimo metodu ravnih valova s pseudopotencijalom, primijenjenu u programu ABINIT, da bismo predvidjeli procijepe energijskih vrpci, elastične konstante i dinamička svojstva rešetaka legure $GaP_xAs_ySb_{1-x-y}$ s četiri sastavnice, priležne na GaAs i InP podloge. Odredili smo područja sastava za koja rešetke priliježu na GaAs i InP. Postigli smo vrlo dobar sklad izračunatih vrijednosti s eksperimentalnim podacima za polazne legure GaAs i $GaAs_{0.5}Sb_{0.5}$. Istražili smo ovisnost izravnih i neizravnih procijepa vrpci o sastavu. Opaža se pojava faznog prijelaza za sadržaj As od 0.018 i 0.576 u $GaP_xAs_ySb_{1-x-y}$ na InP i GaAs podlogama. Statičke i visokofrekventne dielektrične konstante te indeks loma su obrnuto razmjerni (razmjerni) širini osnovnog procijepa vrpci u $GaP_xAs_ySb_{1-x-y}$ na InP and GaAs podlogama. Proučavamo promjene elastičnih konstanti, optičkih fononskih frekvencija (ω_{TO} i ω_{LO}) te Bornovog efektivnog naboja Z^* u ovisnosti o sadržaju As.